Improved Thresholding Method for Cell Image Segmentation Based on Global Homogeneity Information

Kazeem Oyeyemi Oyebode
School of Engineering, Howard College Campus, University of KwaZulu-Natal, Durban South Africa
kazeemkz@gmail.com

***Abstract*—Cell segmentation provides opportunity to highlight abnormalities in the human body with a view to assist medical experts to diagnose objectively. In order to achieve this, a robust segmentation tool that gives high segmentation accuracy is desirable. Cell images can be classified as homogeneous and heterogeneous. Their existence in any of the two categories is a function of how they are captured. This however hinders the deployment of existing segmentation models such as graph cut, Otsu thresholding, k-means and watershed to cater for these categories of cell images. Our contribution in this paper is to develop in the first instance a segmentation model that automatically categorizes cell images as homogeneous and heterogeneous. Secondly, based on a category, a suitable and improved Otsu thresholding method is proposed for cell segmentation. Experimental results on heterogeneous cell images show improved segmentation accuracy of 91.36% over that derived from traditional Otsu thresholding (74%).**

***Index Terms*— Segmentation; Otsu Thresholding; Cell images; Cell Segmentation.**

I. INTRODUCTION

The ability of medical experts to diagnose ailments such as tuberculosis or cancer largely depends on image processing, which plays an important role. It provides a platform where desired objects of interest are projected to the foreground, thereby, providing an opportunity for analysis and diagnosing.

There are many cell segmentation methods in the literature, of which one of them is the thresholding. This segmentation model wholly depends on the intensity of image pixels. It assumes that given an image *M*, the pixels found in *M* have an object region with a distinct intensity level from its background, giving rise to a bimodal histogram. Based on this, a calculated threshold *T* (normally at the valley of the bimodal histogram) is calculated and the image is segmented based on this threshold [1]. Thresholding produces a binary image *B(x; y)* from an image *M(x; y)*, where each pixel found in *B(x; y)* takes either the value 1 or 0 [2] . The simplicity of this method means that it is fast to run on cheap hardware infrastructure. Also, the process can be fully automated with an agreed threshold worked out using a global intensity histogram [1]. Thresholding is one of the common cell segmentation approaches [3]; however, because cell images have varying grey-scale intensity levels, thresholding in general performs poorly. Furthermore, thresholding cells for segmentation does not perform satisfactorily when cell images are non-uniformly illuminated. This is because the valley in the bimodal histogram disappears, which makes it difficult to calculate the threshold *T* that demarcates foreground pixels from background pixels for image segmentation. However, thresholding has been used for several cell segmentation models [4] [5], and [6] . In addition, Otsu [7] proposed an algorithm that automatically generates a threshold *T* for object segmentation where the variability of foreground and background grey level intensities is optimized. In this approach, a global intensity level is worked out which is then used to segment any image into foreground and background. The Otsu threholding still faces challenges when segmenting the heterogeneous cell images as some background pixels have the same intensity level as the foreground.

In addition, the watershed segmentation approach acts on the intensity level of pixels [2]. Here, images are viewed as a landscape where waterfall from this high landscape will naturally settle in regions of lower elevation. The processes of flooding the low landscape areas will naturally segment and isolate regions. These isolated (segmented) high landscapes are referred to as segmented region (s), while the flooded (low landscape) areas form the boundary of segmented region(s). Also, the k-means clustering [8], [9] is a region based approach that partitions images into foreground and background. Where cell images are heterogeneous, the k-means method suffers from severe over-segmentation. The k-means clustering is widely used for cell segmentation as observed in [9], [10], [11] and [12].

The graph cut segmentation model uses a global segmentation strategy to segment images into foreground and background with promising results. It has therefore found application in many cell segmentation problems [13], [14], [15], [16], [17] and [18]. However, the graph cut segmentation does not perform well on heterogeneous cell images. Other methods have also been proposed in the literature for cell image segmentation, such as the merging algorithm [19] where segmentation is carried out on individual sub-images before segmentation output of these sub-images are merged.

The main problem of existing models in the literature is that they are not adaptive in nature to cope with a wide array of cell image presentation. As a result, we propose an improved method based on global homogeneity information which allows the category of a cell image to be determined first (homogenous, and heterogeneous), and thereafter carrying out segmentation.

The rest of the paper is organized as follows: Section II throws light at the proposed model, section III discusses the

experiment carried out on the proposed model. Lastly, section IV concludes the paper.

II. PROPOSED MODEL ON CELL IMAGE SEGMENTATION

This section introduces the proposed cell image segmentation based on global homogeneity information. One of our contributions is to intuitively classify any cell image into homogeneous or heterogeneous cell image and there after segment each one based on their categorization.

$$V_o(x,y) = c * \quad V_i(x,y)^{\partial} \tag{1}$$

First, for the heterogeneous cell images, they are enhanced logarithmically using (1) to give images in Figure 1 (b). In (1), $V_i(x,y)$ is the intensity value of pixel at the location *(x,y)* of the input image. $V_o(x,y)$ indicates the intensity value of pixel at location *(x,y)* of the output image. ∂ (set to 0.4) controls the level of foreground pixel shrinkage [20], and c (set to 2) is the scaling factor. The objective of this stage is to accentuate the global homogeneity of cells. Secondly, an initial Otsu thresholding is carried out, resulting in Figure 1. (c). This is followed by the elimination of cells of a pre-defined size *s* (set to 90000000 pixels) (Figure 1. (d)). The result of the elimination of cells of a given size reveals the nature of the cell image, either as homogeneous or heterogeneous. A cell is homogeneous if a few cells or no cell image (foreground pixels) exists after the elimination of cells below a given size *s* (Figure 2. (d)). However, for heterogeneous cell images, there exist more cells (foreground pixels), above a given threshold, even after the elimination of cells of size *s* (Figure 1. (d)). The existence of foreground pixels, above a threshold, rules out a homogeneous cell image. As a result, a further cell image partitioning is carried out to automatically partition cell images into fairly homogeneous units, as observed in Figure 1 (e). These units are segmented using Otsu thresholding independently before segmented units are merged, as seen in Figure 1 (f).

The discussion put forward above also applies to homogeneous cell images. However, a further cell image partitioning is not needed because after the elimination of cells of a given size *s*, few or no foreground pixel exist (Figure 2. (d)). Therefore, an Otsu thresholding is only carried out on the image in Figure 2. (b) to give Figure 2 (e). Algorithm 1 shows how the proposed segmentation is carried out.

Algorithm 1: Improved Thresholding Method for Cell Image Segmentation Based on Global Homogeneity Information

1: Input: Image *I*
2: Output: Image *A*
3: Logarithmically enhance *I*, save in *E*
4: Perform an initial Otsu thresholding on *E*, save in *O*
5: Isolate cells whose sizes are less than a given size *s*, save result in *S*
6: **If** (the number of pixels in *S* >= *t*)
7: Partition *I* into *P* sub-images
8: **for** each image *p* in *P* **do**
9: Gaussian filter *p*, save result in *g*
10: Carry out Otsu thresholding on *g*, save result in *r*
11: Merge all *r* (from segmented sub-images) into *A*
12: **end for**
13: **else**
14: Gaussian filter *E*, save result in *G*
15: Carry out Otsu thresholding on *G*, save result in *A*
16: **end**

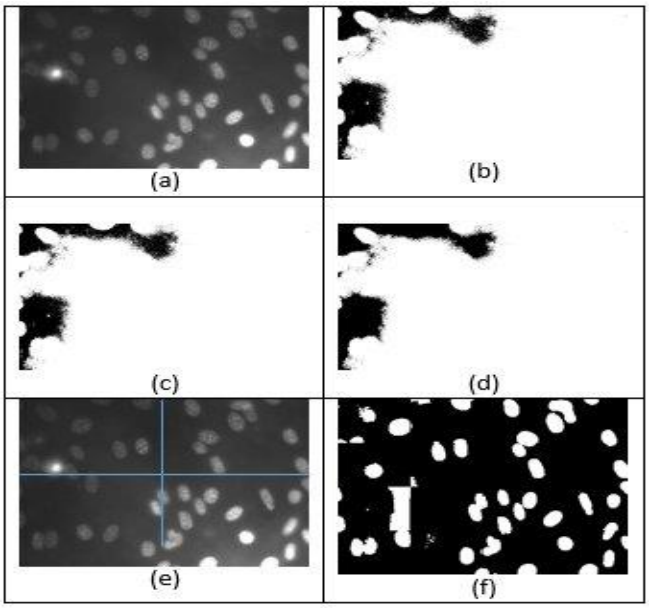

Figure 1: (a) heterogeneous cell image. (b) Logarithmic enhancement of image in (a). (c) Otsu thresholding of image in (b). (d) Isolation of cells of size less than *s* in (c). (e) Partition image in (a) into sub-images, thereafter, carry out Otsu thresholding on each unit. (f) Merged segmented results from each unit into a single image.

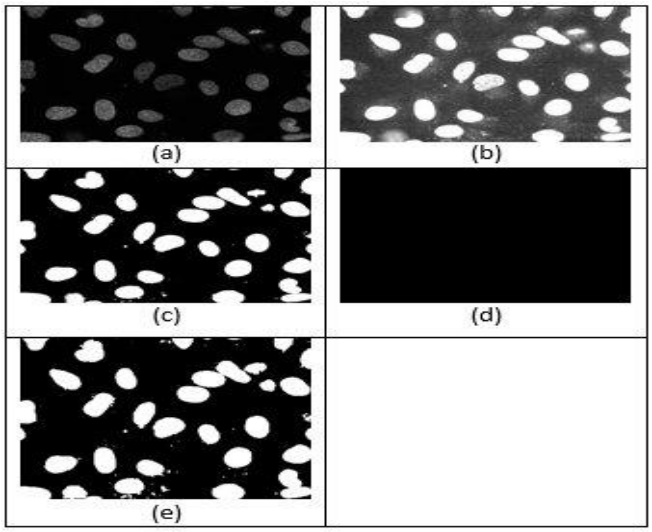

Figure 2: (a) Homogeneous cell image. (b) Logarithmic enhancement of images in (a). (c) Otsu thresholding of image in (b). (d) Isolation of cells of size less than *s* in (c). (e) Otsu segmentation result of image in (b).

III. RESULT AND DISCUSSION

A. Dataset

The proposed model is evaluated using publicly available datasets [19]. These datasets consist of homogeneous and heterogeneous cell images. The homogeneous dataset is named U2OS: It contains 48 images (each image is of size 1349 × 1030) of 1831 cells in total. The heterogeneous dataset is named NIH3T3 and contains 49 images (each image is of size 1344 × 1024) of 2178 cells in total.

B. Parameter Selection

In Eq. (1), c is set to 2 while ∂ is set to 0.4. In Algorithm 1, s is set to 90000000 pixels, t is set to 11000 pixels and P is set to 4.

C. Evaluation and Results

The metrics Accuracy (A) and F-score (F) have been used to evaluate the proposed algorithm. These are given below

$$A\,(\%) = \frac{TP+TN}{(TP+TN+FP+FN)} \tag{2}$$

$$\text{Sensitivity } (\%) = \frac{TP}{(TP+FN)}$$

$$\text{Precision } (\%) = \frac{TP}{(TP+FN)}$$

$$\text{F-score } (\%) = 2 * \frac{(\text{Sensitivity} * \text{Precision})}{(\text{Sensitivity} + \text{Precision})} \tag{3}$$

True positive (TP) is the total number of foreground pixels in the segmented image (SI) that are foreground in the ground truth (G) image. True negative (TN) is the total number of background pixels in SI that are also observed as background pixels in GT. False positive (FP) is the total number of foreground pixels in SI that are observed as background pixels in GT. Lastly, false negative (FN) is the total number of background pixels in SI that are observed as foreground pixels in SI.

Table 1
Segmentation Results on Homogeneous Cell Images (U2OS)

Segmentation Models	A (%)	F-Score (%)
Watershed [19]	91	-
Merging algorithm [19]	96	-
K-means clustering	92.4	84
Otsu thresholding [19]	92	82.5
Graph cut	92.4	84
Proposed Model	94	88.5

Table 2
Segmentation Results on Heterogeneous Cell Images (NIH3T3)

Segmentation Models	A (%)	F-Score (%)
Otsu Thresholding [19]	74	-
Watershed [19]	78	-
Merging algorithm [19]	83	-
K-means clustering	83	38
Graph cut	87.28	73.00
Proposed Model	91.36	78.5

D. Discussion

As observed in Table 2, the proposed model demonstrates improved segmentation accuracy (A) over existing models such as the graph cut, watershed, merging algorithm and the thresholding. This implies that the model is able to identify that the cell image is heterogeneous in nature; hence, needs further partitioning. Each partitioned sub-image (homogeneous) is segmented in isolation before they are merged. However, for the homogeneous cell segmentation as observed in Table 1, the segmentation accuracy (A) of the proposed model is the second best. One can attribute this to the logarithmic transformation carried out before segmentation. This may have increased the number of FP pixels, thereby reducing its accuracy.

IV. CONCLUSION

The proposed model provides a platform for segmenting both homogeneous and heterogeneous cells images. However, as observed, the proposed model performs better on heterogeneous cells as compared to homogeneous cells. One can attribute this (of heterogeneous cells) to the partitioning of cell images into sub-images before segmentation is carried out.

REFERENCES

[1] E. Meijering, "Cell segmentation:50 years down the road," IEEE Signal Processing Magazine, 29, (5), (2012) 140-145.

[2] C. Solomon and T. Breckon, "Fundamentals of Digital Image Processing. A Practical Approach with Examples in Matlab", Wiley-Blackwell, 2011.

[3] Q. Wu, F. Merchant, and K. Castleman, "Microscope Image Processing", Elsevier, 2008.

[4] A. A. Nawandhar, L. Yamujala, and N. Kumar, "Image segmentation using thresholding for cell nuclei detection of colon tissue," in International Conference on Advances in Computing, Communications and Informatics, (2015), 1199-1203.

[5] J. W. Xu, T. D. Pham, and X. Zhou, "A double thresholding method for cancer stem cell detection," in 7th International Symposium on Image and Signal Processing and Analysis (ISPA), (2011), 695-699.

[6] H. Madhloom, S. Kareem, H. Ariffin, A. Zaidan, H. Alanazi, and B. Zaidan,"An automated white blood cell nucleus localization and segmentation using image arithmetic and automatic threshold," Journal of Applied Sciences, 10 (11), (2010), 959-966.

[7] N. Otsu, "A threshold selection method from gray-level histograms," IEEE Transactions on Systems, Man, and Cybernetics, 9(1), 1979, 62-66.

[8] J. Hartigan and M. Wong, "A k-means clustering algorithm," the Royal Statistical Society. Series C (Applied Statistics), 28(1), (1979),100- 108.

[9] M. Yan, J. Cai, J. Gao, and L. Luo, "K-means cluster algorithm based on color image enhancement for cell segmentation," in 5th International Conference on Biomedical Engineering and Informatics (BMEI), 2012.

[10] N. M. Salem, "Segmentation of white blood cells from microscopic images using k-means clustering," in 31st National Radio Science Conference, 2014, 371-376.

[11] A. A. Nasir, M. Mashor, and Z. Mohamed, "Segmentation based approach for detection of malaria parasites using moving k-means clustering," in IEEE Conference on Biomedical Engineering and Sciences (IECBES), 2012, 653-658.

[12] L. Bradbury and J. W. L. Wan, "A spectral k-means approach to bright-field cell image segmentation," in International Conference of the IEEE, Engineering in Medicine and Biology Society (EMBC), 2010, 4748-4751

[13] L. Zhang, H. Kong, C. T. Chin, S. Liu, T. Wang, and S. Chen,, "Automated segmentation of abnormal cervical cells using global and local graph cuts," in IEEE 11th International Symposium on Biomedical Imaging (ISBI), 2014, 485 488.

[14] M. Beheshti, J. Faichney, and A. Gharipour, "Bio-cell image segmentation using Bayes graph-cut mode," in International Conference on Digital Image Computing: Techniques and Applications (DICTA), 2015, 1-5, 2015.

[15] R. Bensch and O. Ronneberger,, "Cell segmentation and tracking in phase contrast images using graph cut with asymmetric boundary costs," in IEEE 12th International Symposium on Biomedical Imaging (ISBI), 2015, 1220 -1223.

[16] S. Dimopoulos, C. Mayer, F. Rudolf, and J. Stelling, "Accurate cell segmentation in microscopy images using membrane patterns," Bioinformatics, 30(18), 2014, 2644-2651.

[17] R. Kechichian, H. Gong, M. Revenu, O. Lezoray, and M. Desvignes,, "New data model for graph-cut segmentation:application

to automatic melanoma delineation," in IEEE International Conference on Image Processing (ICIP), 2014, 3188-3191.

[18] Oyebode K.O and Jules Raymond-Tapamo, " Adaptive Parameter Selection for Graph Cut Based Cell Segmentation," Image Analysis and Stereology, vol. 30(1), 2016, 29-37.

[19] Coelho, Luis Pedro and Shariff, Aabid and Murphy, Robert F., "Nuclear segmentationtation in microscope cell images: a hand-segmented dataset and comparison of algorithms," in IEEE International Symposium on Biomedical Imaging: From Nano to Macro, 2009.

[20] N. Mohd Saad, S.A.R. Abu-Bakar, Sobri Muda, M. Mokji, A.R.Abdullah, "Fully Automatic Region Growing Segmentation of Brain Lesion in Diffusion-Weighted MRI," IAENG International Journal of Computer Science, 39 (2), 2012, 155-164.